보건학석사 학위논문

The effect of *Roseburia* spp. in alcoholic liver diseases and epithelial barrier in the gut

로제부리아 균주의 알코올성 간질환과 장내 방벽에 대한 효과

2019년 2월

서울대학교 보건대학원

환경보건학과 환경보건학 전공

전 경 찬

Abstract

The effect of *Roseburia* spp. in alcoholic liver diseases and epithelial barrier in the gut

Jeon kyungchan

Dept. of Environmental Health

The Graduate School of Public Health

Seoul National University

The pathogenesis of alcoholic liver disease (ALD) is related to translocation of endotoxin from alcohol-induced leaky gut to liver, and such a pathway is called gut-liver axis. Therefore, it is important for ALD patients to protect gut barrier against alcohol damage. It has been widely reported that gut microbiota is able to improve gut barrier integrity in various pathological conditions. However, there has been few studies on

effects of individual gut commensals on improving gut barrier function in ALD. In this study, we observed that the abundance of *Roseburia* is reduced in gut and correlated with transcriptional expression levels of intestinal tight junction-related genes (Occludin and Claudin-2) in ALD mice. We, thus, hypothesized that *Roseburia* plays a potential role in regulation of gut barrier integrity in ethanol-damaged condition, thereby associating with ALD. To understand strain-dependent properties of *Roseburia*, characteristics of three *Roseburia* spp. (*R. intestinalis, R. hominis*, and *R. faecis*) were examined, showing strain specificity in both rate of butyrate production and size of flagellin protein. To identify effects of *Roseburia* on strengthening gut barrier, *in vitro* experiments were performed on human epithelial Caco-2 cell line. The treatments of live *Roseburia* spp. at $10^8, 10^9$cells/well for 24h resulted in about 1.2-1.4 fold increase in relative TEER change, and normalized FITC permeability after subsequent ethanol challenge. Furthermore, their supernatants, which contain butyrate as metabolites, were investigated, but not able to improve gut barrier dysfunction. Interestingly, however, treatments of flagellin extracts derived from *R. intestinalis* and *R. hominis* at 250μg/ml improved TEER value and ethanol-induced hyper-permeability to the same extent with treatment of live *Roseburia*,

whereas that of *R. faecis* had no effect. Consequently, *Roseburia* had a beneficial effect on improving ethanol-induced gut barrier dysfunction and their flagellin would be involved in this effect with a strain-dependent variation. These findings proposed *Roseburia* as a novel probiotic target for alleviating ALD.

Key words: *Roseburia*, Alcoholic liver disease (ALD), flagellin, butyrate, Caco-2, ethanol, tight junction, microbiota

Student No. 2017-29583

CONTENTS

List of Tables

List of Figures

I. Introduction

Alcoholic liver disease (ALD) is a consequence of excess alcohol consumption, starting from steatosis to fibrosis, hepatitis, and cirrhosis, serially. Hepatic inflammation basically occurs in every stage of the disease [1]. Recently, one of the causes of ALD was suggested as Gut-Liver-TLR4 axis, in which hepatic inflammation gets involved [2]. Alcohol consumption leads to intestinal barrier dysfunction and increases permeability. Consequently, a variety of luminal antigens, such as endotoxins and bacteria, are directly translocated into the liver via portal vein and contribute to hepatic inflammation through the activation of Toll-like receptor 4 (TLR4) signaling [3]. Therefore, maintenance of gut barrier function is the key to alleviating ALD.

Gut microbiota has been widely accepted to play a crucial role in the pathology of various diseases in skin, lung, and even brain [4]. Among them, the liver disease is highly associated with altered gut microbiota composition because microbial products can be transferred into the liver directly through portal circulation during gut barrier dysfunction [5]. *Ece A. Mutlu et al.* demonstrated that the patients with ALD had low abundance of *Bacteroidetes* and high abundance of *Proteobateria*, which were correlated with high serum levels of endotoxins [6]. By contrast, some of microbiota improve gut barrier dysfunction in ALD. For

instance, administration of *Lactobacillus* spp. ameliorated ALD *in vivo* by enhancing intestinal barrier and reducing serum endotoxin levels [7, 8]. However, there has been few studies on functions of other commensals in alcohol-damaged intestinal condition. It is, therefore, important to figure out the roles of other commensals in ALD pathology to deeply understand the relationship between gut microbiota and the pathology of the disease.

Intestinal tight junction is a complex of junctional proteins, such as Zonula occluden-1 (Zo-1), Occludin and Claudins. It regulates the passage of gut-derived substance through the paracellular pathway in between intestinal epithelial cells [9]. However, ethanol consumption can disrupt tight junction and also down-regulate the transcriptional expression levels of the tight junction-related genes, increasing intestinal permeability [7, 10]. To investigate gut barrier function in the epithelial cells, human colon carcinoma Caco-2 cell line model has been adopted [11, 12]. In particular, the Caco-2 model was used in ethanol-damaged condition in order to simulate the gut barrier dysfunction of alcoholics [13]. Although the effects of gut microbes as well as their metabolites on ethanol-damaged intestinal tight junction have been studied, the cell components, such as flagellin, have not been examined as an effector molecule on improving Caco-2 tight junction.

Roseburia is a member of the phylum Firmicutes and Gram-positive anaerobic bacteria that resides in human colon. *Roseburia* has following characteristics: 1) producing butyrate, 2) motile by means of multiple subterminal flagella, 3) associated with various metabolic diseases such as obesity and colitis [14]. Butyrate is one of the short chain fatty acids (SCFAs), which serve as a main energy source of epithelial cells, and strengthen intestinal tight junction [15]. *Roseburia intestinalis*-derived flagellin was recently studied on the anti-inflammatory properties by regulating host HIF1α-AS gene expression on Caco-2 cells [16]. Furthermore, *Roseburia hominis* was associated with alcohol resistant mice compared to the sensitive one, and *Lachnospiraceae* including *Roseburia* was reduced in cirrhotic and alcoholic patients [17]. However, the specific health effects of *Roseburia* in alcohol-damaged condition and its strain-dependent variation are not fully understood.

In this study, we observed the association of the abundance of *Roseburia* with alcohol consumption and intestinal tight junction related gene expression using *in vivo* ALD mouse model fed Lieber-DeCarli diet. Therefore, the aim of the study was to investigate the improving effects of *Roseburia* on ethanol-induced barrier dysfunction and figure out their strain-specificity. Three of *Roseburia* spp. were chosen and compared

the characteristics to understand strain-dependent efficacies. The live bacteria, the supernatant and flagellin extracts were examined on Caco-2 monolayer as potential targets of interest. Thus, we demonstrated that *Roseburia*-derived flagellin has a beneficial role in enhancing tight junction, and *Roseburia* can be used as probiotics on alcohol-damaged intestinal barrier dysfunction.

II. Materials and Methods

1 Bacteria culture and preparation

Roseburia intestinalis SNUG30017, *Roseburia faecis* SNUG33007 and *Lactobacillus ruminis* SNUG30021 were isolated from fecal samples of healthy adult Korean. *Roseburia hominis* A2-183 was purchased from DSMZ (Deutsche Sammlung von Mikroorganismen und Zellkulturen). *Roseburia* was cultured on YBHI medium at 37℃ under anaerobic condition as described in previous study [20]. *Lactobacillus* was cultivated on Lactobacilli MRS medium supplemented with 0.05% L-cysteine-hydrochloride in the same condition. In order to harvest bacteria cells, culture media were centrifuged at 8,000 x g at 4℃, and washed twice with sterile anaerobic PBS, and resuspended in it. After then, live bacteria were counted with Accuri C6 Flow Cytometer (BD Biosciences, Franklin Lakes, NJ) using the Live/dead Baclight viability and counting kit (Molecular Probes, Eugene, OR).

2 Experimental Alcoholic liver disease *in vivo*

Eight weeks old male C57BL/6 mice was obtained from the Central Lab Animals Incorporation. Animal experimental procedure was approved by the Institutional Animal Care and Use Committee (IACUC) of Seoul National University, Korea (Case Number: SNU-170103-9). For experimental ALD mouse model, mice was fed Lieber-DeCarli diet *ad libitum* (Bio-Serv, [18]). Briefly, after acclimatization to a semiliquid diet for 2days, ethanol-fed group received increasingly higher dose of ethanol (1% and 3% every 2days; v/v). The final ethanol concentration was 5% for 10days, whereas pair-fed group received an isocaloric amount of maltodextrin. Body weights and food intake were checked every day and these were comparable with each groups (data not shown). To investigate intestinal permeability, fluorescein isothiocyanate (FITC)-dextran (4 kDa; Sigma-Aldrich) was orally administrated (60mg/100g body weight) 4h before sacrifice on day 16. After sacrificed, blood samples were collected in EDTA-coated tubes and immediately centrifuged (5,000 x g, 4℃) for 10min to isolate sera. Fluorescence was measured with spectrophotometer (TECAN) at an excitation wavelength of 485nm and emission wavelength of 528nm. In addition to blood, both liver and small intestine were collected for further analysis.

3 Biochemical assays

Serum ALT activity was quantified with the EnzyChrom Alanine Transaminase Assay kit (BioAssay Systems, Hayward, CA), and serum AST was measured with the EnzyChrom Aspartate Transaminase Assay kit (BioAssay Systems) following the manufacturer's instructions. For hepatic TG quantification, total lipids were extracted from the liver tissue as widely-used Folch method [19] and quantified with the EnzyChrom Triglyceride Assay kit (BioAssay Systems). To determine serum LPS levels, Limulus Amebocyte Lysate Assay kit (Lonza, Basel, Switzerland) was used according to manufacterer's manual.

4 Histological analysis

To visualize alcoholic liver lesion, liver tissue was dyed with hematoxylin and eosin (H&E). Liver tissue was fixed in 10% formalin, and paraffin-embedded section was stained with H&E.

5 Microbiota composition analysis

Total genomic DNA was extracted from cecum contents with QIAmp Fast DNA stool mini kit (Qiagen). The V3-4 region of 16S rRNA gene was amplified with general bacterial primers 341F (CCTACGGGNGGCWGCAG) and 805R (GACTACHVGGGTATCTAATCC). PCR amplicons were purified using QIAquick PCR Purification Kit (Qiagen) and sequenced with a MiSeq platform (illumina. Inc., San Diego, CA, USA). Raw FASTQ files were demultiplexed and quality filtered, and data was processed by using Quantitative Insights into Microbial Ecology (QIIME) 1.8.0 software (QIIME development team; website: http://qiime.org/). The sequences were clustered into operational taxonomic units (OTUs) using an open-reference OUT picking and representative sequence sets were picked using UCLUST. The relative abundance of microbial taxa genus to kingdom was generated from nonrarefied OTU table. For taxonomic assignment, the OTUs were aligned using PyNAST and compared with the Greengenes reference 16S rRNA gene database preclustered at 97% identity (release gg_13_5.fasta). Chimera checking was performed using ChimeraSlayer. After removing singletons, rare OTUs found in fewer than 10% of the samples were excluded, and 9,000 OTUs were observed.

6 Quantitative real-time PCR (qRT PCR)

In order to measure mRNA expression levels of tight junction-related genes, quantitative real-time PCR was performed. Intestinal tissue was immediately brought into RNAlater (Thermo Fisher Scientific, Waltham, MA) and stored at -80℃. Frozen tissue was homogenized in lysis buffer using MM 400 Mixer Mill homogenizer (Retsch, GmbH., Haan, Germany). RNA was isolated using an easy-spin total RNA extraction kit (iNtRON Biotechnology Inc., Seoul, Korea). Total RNA concentration was measured with NanoDrop Spectrophotometer ND-1000 (Thermo Fisher Scientific), and RNA was reversely transcribed to cDNA using High Capacity RNA-to-cDNA kit (Applied Biosystems, Foster City, CA). qRT PCR was achieved using the Rotor-Gene Q using the QuantiTect SYBR Green PCR kit (Qiagen). The sets of primer used were listed in Table 1. Relative gene expression was normalized to hypoxanthine-guanine phosphoribosyltransferase (HPRT). To quantify the amount of *Roseburia* in stool sample, *Roseburia*-specific sequence was amplified in total genomic DNA in fecal samples and detected by qRT PCR as previously studied [20].

Table 1. PCR primers

Target	Sequence (from 5′ to 3′)		Reference
HPRT	Forward	TTATGGACAGGACTGAAAGAC	[21]
	Reverse	GCTTTAATGTAATCCAGCAGGT	
Zo-1	Forward	ACCCGAAACTGATGCTGTGGATAG	[17]
	Reverse	AAATGGCCGGGCAGAACTTGTGTA	
Occludin	Forward	GGAGGACTGGGTCAGGGAATA	[17]
	Reverse	CGTCGTCTAGTTCTGCCTGT	
Claudin-2	Forward	GGCTGTTAGGCACATCCAT	[22]
	Reverse	TGGCACCAACATAGGAACTC	
Claudin-3	Forward	CAGACGTCCGTCAGTTTTCG	[17]
	Reverse	CATGGCTGCTGGACTTGAAC	
Claudin-4	Forward	ACTTTTTGTGGTCACCGACT	[17]
	Reverse	GCGAGCATCGAGTCGTACAT	
Roseburia-specific sequence	Forward	CGKACTAGAGTGTCGGAGG	[20]
	Reverse	GTCATCTAGAGTGTCGGAGG	

7 *Roseburia* characterization

Bacterial genomic DNA was extracted using Wizard genomic purification kit (Promega Corporation, Madison, WI). Bacterial 16S rRNA genes of *R. intestinalis* SNUG30017 and *R. faecis* SNUG33007 were sequenced. To investigate phylogenetic distance, 16S rRNA gene sequences of related type strains were obtained from EzTaxon database and aligned using EzEditor program. Phylogenetic relationships were inferred on 1430 shared nucleotides based on neighbor-joining method using the MEGA program version 7.0.26. Evolutionary distances were computed as Juke & Cantor's one-parameter model and the stability of the clustering was estimated by bootstrap analysis with 1,000 replications. All process of phylogenetic analysis were based on published paper [23].

R. intestinalis SNUG30017, *R. faecis* SNUG33007 and *R. hominis* A2-183 were cultured in broth. Supernatants were collected every three hours, subsequently measured optical density at 600nm using a spectrophotometer (TECAN) to set growth curves up, and stored at -80℃ for gas chromatography. In order to measure butyrate production rate, frozen supernatants were analyzed using a GC flame ionization detector (FID) system as previously described [24]. 1% 2-methyl pentanoic acid (Sigma-Aldrich) was used as the internal standard.

Cell morphology and presence of flagellin was determined by transmission electron microscopy with negative staining method.

8 Flagellin extraction

The flagellin extracts was prepared as described previously [16]. Briefly, *R. intestinalis* SNUG30017, *R. faecis* SNUG33007 and *R. hominis* A2-183 were incubated in broth. Cells were removed from the culture medium by centrifugation at 1,750 x g at 4°C for 20 min and resuspended in cold PBS. The cell suspensions were blended to isolate the flagella from the cell surface. The homogenization was repeated three times on ice prior to centrifugation at 10,000 x g at 4°C for 20 min. The supernatants were ultracentrifuged (Beckman Coulter, Brea, CA) at 100,000 x g at 4°C for 1 h to concentrate the crude flagellin proteins. The crude proteins were resuspended in triple-distilled water. The protein fraction was loaded on an SDS-PAGE gel.

9 Caco-2 cell culture and ethanol-damaged *in vitro* model

Caco-2 cells were collected from the American Type Culture Collection (ATCC) and maintained in Minimum Essential Medium (MEM; Gibco, Grand Island, NY) supplemented with 20% fetal bovine serum (FBS; GenDEPOT, Barker, TX), 1% nonessential amino acids, 1% HEPES, 1.5% sodium bicarbonate solution, 50 μg/ml of gentamicin and 10 U/ml of penicillin-streptomycin at 37°C in a 5% CO2 environment. Caco-2 cells were subcultured every 7 days and used at passages 35-42. The cells were seeded onto Transwell inserts (Corning Inc., Corning, NY) at a density of 3×10^4 cells/well and differentiated for 7 days. Following starvation of polarized Caco-2 overnight, live bacteria, supernatant, and flagellin extract were treated for 24h in distinct sets of experiment. *Roseburia* live bacterial cells were prepared and co-cultured at a density of 1×10^8 or 1×10^9 cells/well. The supernatants were supplemented in culture medium at a 1% (v/v) after 0.22-μm filtration. Flagellin extracts were treated at 250 or 500 μg/ml concentration. The integrity of the differentiated cells was measured as the transepithelial/transendothelial electrical resistance (TEER) value using an EVOM epithelial voltohmmeter (World Precision Instruments, Sarasota, FL) at 0 h and 24 h after bacterial cell treatment. To determine the protective effect of the bacterial cells against alcohol challenge,

ethanol was administrated at 3%(v/v)/well to the basolateral region and incubated for 3h. The ethanol was changed every hour to compensate for evaporation. The permeability of ethanol-damaged Caco-2 monolayer was quantified by adding FITC-dextran into the apical region at a 1 g/l concentration. After incubation for an hour, fluorescence from the basolateral culture medium was detected using a spectrophotometer (TECAN) at an excitation wavelength of 485 nm and emission wavelength of 528 nm. Sodium butyrate was compared as a positive control (1% of 2mM concentration) for TEER upregulation both in the normal and ethanol-damaged condition [13, 25].

10 Cell viability test

Caco-2 cell was cultured on 96well plate for 24h. After starvation overnight, ethanol was challenged at 0-10% concentration with 2% intervals for 3h. Cell viability was examined using the MTT (3-(4,5-Dimethylthiazol-2-yl)-2,5-Diphenyltetrazolium Bromide) assay. Briefly, 5mg/ml MTT in PBS was added to each well and incubated for 1h at 37℃. The media were then removed and formazan crystals in the cells were dissolved in the presence of dimethyl sulfoxide. The plates were read at 590nm wavelength using a spectrophotometer (TECAN). The percentage of cell viability was calculated by comparing the optical densities of the cells treated with different concentrations of ethanol with that of the control.

11 Western blot

Caco-2 cell was cultured on 6well plate for 7days. After starvation overnight, ethanol was challenged at 0-8% concentration for 3h. Cells were harvested and centrifuge at 850 x g for 10min. After remove supernatant, the pellet was reconstituted in RIPA buffer with Halt™ Protease Inhibitor Cocktail (100X) (78438, Thermo Fisher Scientific) and vortexed 3 times for 10sec with intervals of 5min on ice. Protein was quantified with Pierce™ BCA Protein Assay Kit (23225, Thermo Fisher Scientific). Lysates were solubilized in Laemmli sample loading buffer (Bio-Rad Laboratories Inc., Hercules, CA) with 10% β-mercaptoethanol and boiled for 10 min at 85°C. Samples with equal amounts of protein were separated on a 10% SDS-PAGE gel and transferred onto a nitrocellulose membrane. Then, the membranes were blocked for 1 h in 5% BSA in TBS containing 0.1% Tween 20 and incubated overnight at 4°C with the following specific primary antibodies: mouse monoclonal anti-β-actin (A5441, Sigma-Aldrich) and mouse monoclonal anti-occludin (33-1500, Thermo Fisher Scientific). After repeated washing, the membranes were incubated with corresponding horseradish peroxidase-labeled secondary antibodies (Thermo Fisher Scientific) for 1 h. The protein bands were visualized using an enhanced chemiluminescence reaction (170-5060, Bio-Rad Laboratories Inc.) and

exposed to Geldak film (Syngene International Ltd., Bengaluru, India) at an optimized time point. The relative signal intensity was quantified with GeneTools (Syngene International Ltd.).

12 Statistical analysis

Data are expressed as means ± standard error of the mean (SEM). GraphPad Prism 5.04 (GraphPad Software, Inc., La Jolla, CA) was used to visualize and analyze all other data using t-test. Statistical significance was given as '*' $p < 0.05$, '**' $p < 0.01$, '***' $p < 0.001$.

III. Results

1. Alcohol consumption induced alcoholic liver disease (ALD) in mice

To investigate the effect of alcohol consumption, mice was fed Lieber-DeCarli diet with increasingly elevated concentrations of ethanol for 15days (Fig. 1A). Ethanol consumption considerably increased lipid droplets and neutrophil infiltration in the liver as shown in H&E staining, demonstrating steatosis and inflammation (Fig. 1B). Also, AST and ALT levels in serum and hepatic triglycerides levels were significantly increased (Fig. 1C-E). Accordingly, it is obvious that alcohol consumption induced alcoholic liver disease (ALD) in mice.

In order to test gut permeability, FITC-dextran was administrated 4h before sacrifice and fluorescence was measured in serum. Fluorescence was substantially detected in serum from ethanol-fed group, indicating gut barrier dysfunction (Fig. 1F). It allowed microbial antigens to pass through intestinal barrier and may resulted in hepatic inflammation. Enhanced levels of LPS in serum confirmed disrupted gut barrier function and clearly showed endotoxemia (Fig. 1G).

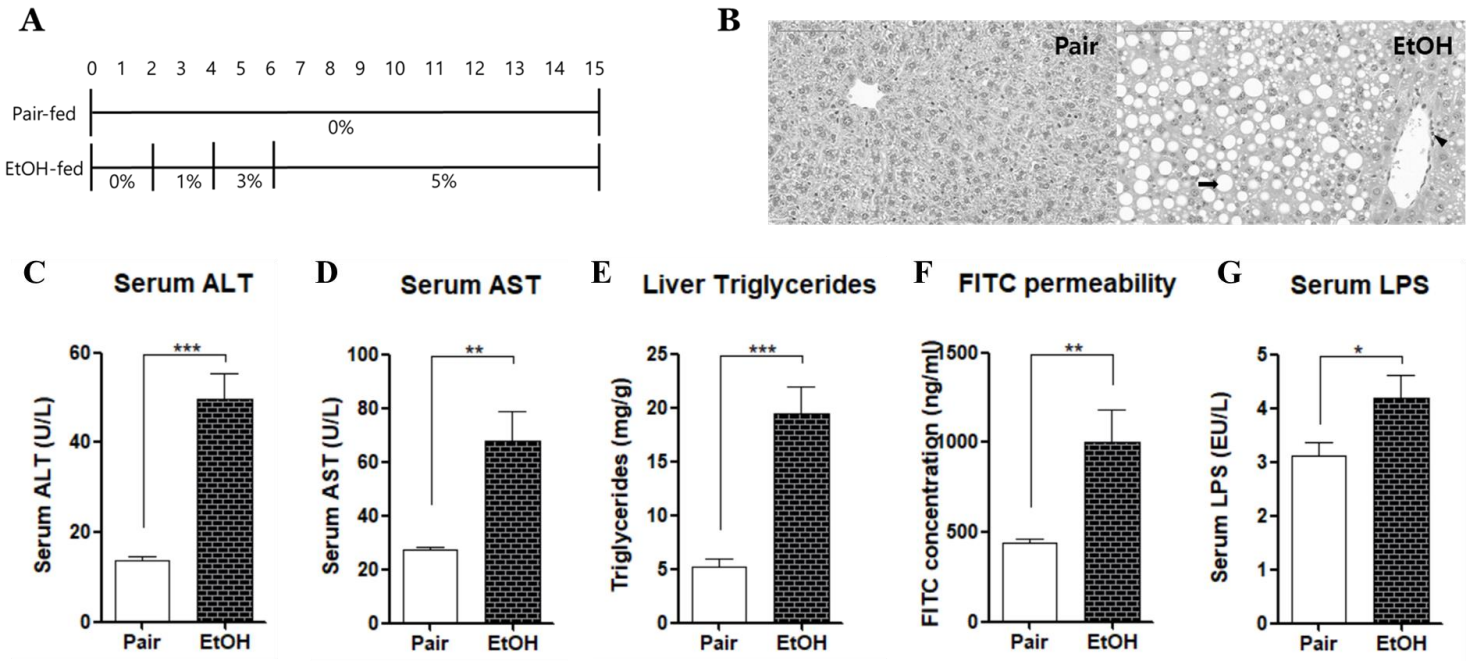
A
0 1 2 3 4 5 6 7 8 9 10 11 12 13 14 15
Pair-fed
0%
EtOH-fed
0%
1%
3%
5%
B
Pair
EtOH
C
Serum ALT
Serum ALT (U/L)
***
Pair
EtOH
D
Serum AST
Serum AST (U/L)
**
Pair
EtOH
E
Liver Triglycerides
Triglycerides (mg/g)
***
Pair
EtOH
F
FITC permeability
FITC concentration (ng/ml)
**
Pair
EtOH
G
Serum LPS
Serum LPS (EU/L)
*
Pair
EtOH

Figure 1. Alcohol consumption induced alcoholic liver disease (ALD) in mice.

(A) C57BL/6 male mouse were fed an alcohol Lieber DeCarli diet for 15days, whereas pair-fed group additionally received an isocaloric amount of maltodextrin without alcohol (n=8 per group). Major markers for ALD were compared between pair and ethanol-fed group). (B) H&E staining of the liver lesion; black arrow indicates lipid droplets and black triangle points neutrophil infiltration, (C) Serum ALT, (D) Serum AST, (E) Hepatic triglycerides(TG) levels. Intestinal permeability was measured as (F) FITC-dextran fluorescence and (G) Serum LPS levels. Statistical analysis was performed using t test and error bars represent SEM. *, $P < 0.05$; **, $P < 0.01$; ***, $P < 0.001$.

2. Alcohol consumption altered gut microbial composition and relative abundance of family *Lachnospiraceae* was considerably enriched in pair-fed group.

Recently, it has been widely reported that gut microbiota composition was associated with alcohol-induced gut barrier dysfunction [5, 6]. We investigated altered gut microbiota composition to find out possible microbiota associated with gut barrier dysfunction in ALD. Alcohol consumption led to reduced alpha diversity based on phylogenetic distance in the microbial community of ethanol-fed group (Fig. 2A). Also, beta diversity analysis using an unweighted UniFrac distance matrix showed great alterations in the microbial composition by alcohol consumption (Fig. 2B). It indicated that alcohol consumption resulted in gut microbial dysbiosis.

We next compared taxonomic shifts in gut microbial communities using univariate analysis to find individual taxa altered by ethanol consumption (Fig. 2C). In pair-fed group, phylum Firmicutes and its family *Lachnospiraceae* were significantly increased compared to ethanol-fed group. Therefore, we focused on the family *Lachnospiraceae* as a target associated with gut barrier function in ethanol-damaged condition, since the member of the family has been studied as

regulating intestinal homeostasis in humans by producing butyric acid [26].

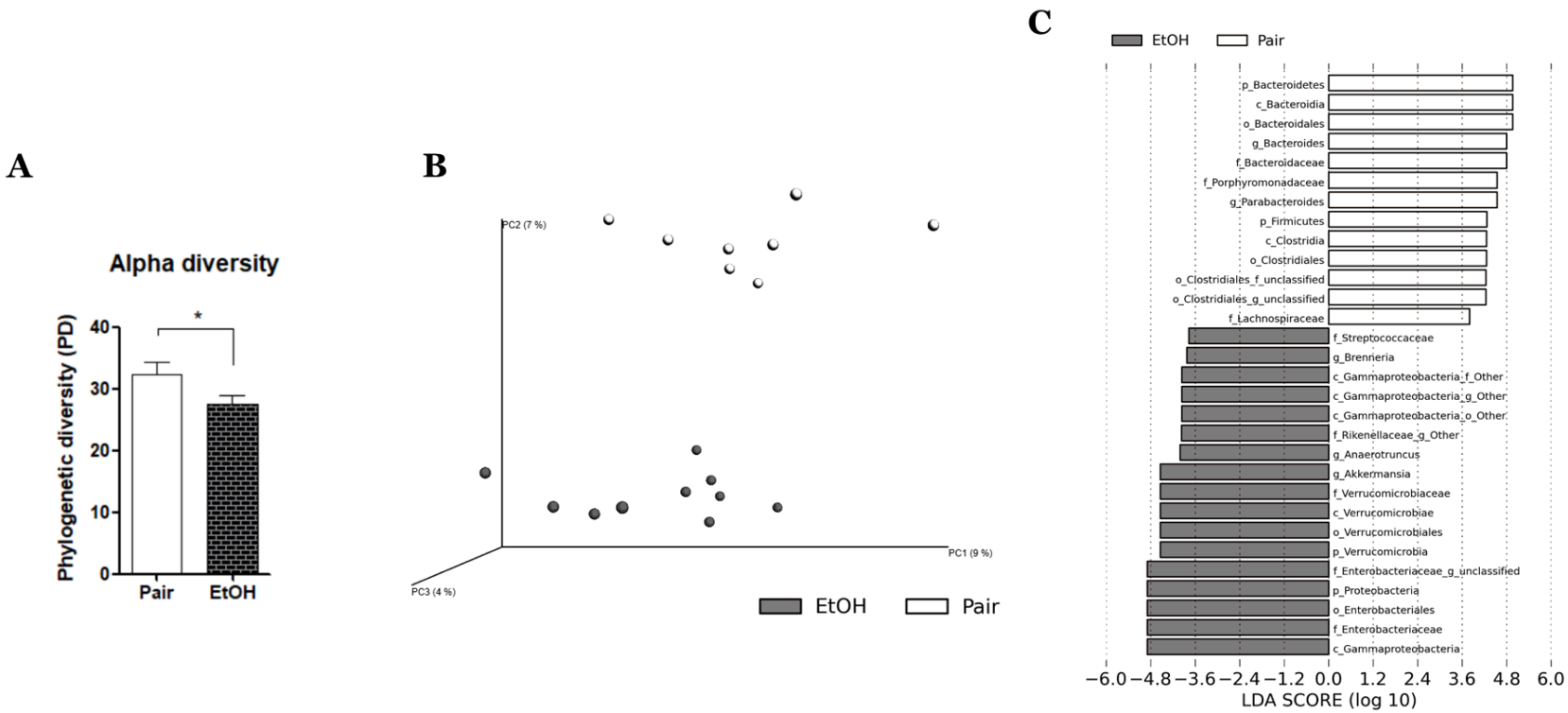
A
Alpha diversity
Phylogenetic diversity (PD)
40
30
20
10
0
*
Pair
EtOH
B
PC2 (7 %)
PC1 (9 %)
PC3 (4 %)
EtOH
Pair
C
EtOH
Pair
p_Bacteroidetes
c_Bacteroidia
o_Bacteroidales
g_Bacteroides
f_Bacteroidaceae
f_Porphyromonadaceae
g_Parabacteroides
p_Firmicutes
c_Clostridia
o_Clostridiales
o_Clostridiales_f_unclassified
o_Clostridiales_g_unclassified
f_Lachnospiraceae
f_Streptococcaceae
g_Brenneria
c_Gammaproteobacteria_f_Other
c_Gammaproteobacteria_g_Other
c_Gammaproteobacteria_o_Other
f_Rikenellaceae_g_Other
g_Anaerotruncus
g_Akkermansia
f_Verrucomicrobiaceae
c_Verrucomicrobiae
o_Verrucomicrobiales
p_Verrucomicrobia
f_Enterobacteriaceae_g_unclassified
p_Proteobacteria
o_Enterobacteriales
f_Enterobacteriaceae
c_Gammaproteobacteria
−6.0 −4.8 −3.6 −2.4 −1.2 0.0 1.2 2.4 3.6 4.8 6.0
LDA SCORE (log 10)

Figure 2. Alcohol consumption altered gut microbial composition and relative abundance of family *Lachnospiraceae* was considerably enriched in pair-fed group.

(A) Alpha diversity based on phylogenetic distance (PD) index was significantly decreased in ethanol-fed group. (B) 3D PCoA plot using the unweighted UniFrac distance matrix showed distinct distribution in each group. (C) Significantly different taxa were determined by LEfSe with a sequentially significant ranking (p-value < 0.05) in both the Kruskal-Wallis test among classes and Wilcoxon′s test between subclasses. The threshold for the logarithmic LDA scores was 3.75. Statistical analysis in alpha diversity was performed using one-tailed t test error bars represent SEM. *, P < 0.05.

3. The abundance of genus *Roseburia* was correlated with intestinal transcriptional expression levels of tight junction-related genes in mice

In the family *Lachnospiraceae*, genus *Roseburia* has been focused on its association with metabolic disease [14]. Likewise, we examined the relative abundance of *Roseburia* in fecal samples of both groups using qRT PCR (Fig. 3A). Indeed, the relative abundance of *Roseburia* was significantly reduced in ethanol-fed group. Next, to identify an association between the abundance of *Roseburia* and gut barrier function, relative transcriptional expression levels of tight junction-related genes in small intestine were measured (Fig. 3B). It was found that the levels of Occludin were significantly down-regulated, whereas those of Claudin-2 and Claudin-3 were up-regulated in ethanol-fed group (Fig. 3B). It demonstrated that alcohol consumption affected intestinal epithelial barrier function by perturbing transcriptional expression levels, especially in tight junction-related genes. To investigate correlation between relative *Roseburia* abundance and the transcriptional expression levels of tight junction-related genes, heat map was constructed (Fig. 3C). Significant and positive correlation was detected on Occludin expression, and negative one was shown on Claudin-2 expression (Fig 3B). Therefore, it is suggested that *Roseburia* had a potential role in regulating

intestinal epithelial barrier function.

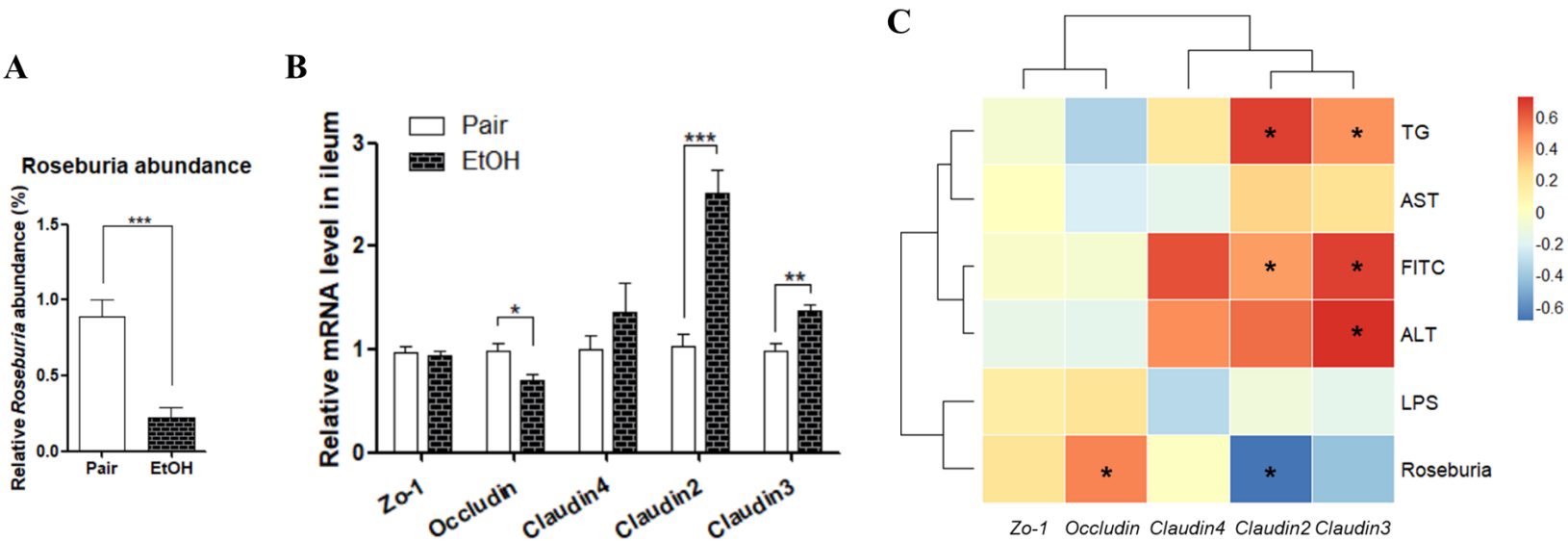
A
Roseburia abundance
Relative Roseburia abundance (%)
1.5
1.0
0.5
0.0
***
Pair
EtOH
B
Relative mRNA level in ileum
3
2
1
0
Pair
EtOH
*
***
**
Zo-1
Occludin
Claudin4
Claudin2
Claudin3
C
TG
AST
FITC
ALT
LPS
Roseburia
Zo-1
Occludin
Claudin4
Claudin2
Claudin3
0.6
0.4
0.2
0
-0.2
-0.4
-0.6

Figure 3. The abundance of genus *Roseburia* in fecal samples was significantly decreased in ethanol-fed group and intestinal mRNA expressions of tight junction-related genes were correlated with the abundance

(A) The abundance of genus *Roseburia* was measured in mouse fecal samples by using qRT-PCR quantification with *Roseburia*-specific primer set. (B) Intestinal mRNA expression levels of tight junction-related genes were calculated with qRT-PCR. Primers were listed on Table 1. (C) Heatmap represented Spearman′s correlation between two parameters; rows are mRNA expression levels of 5 tight junction-related genes, and columns are 5 ALD related markers and the abundance of *Roseburia* in fecal sample. Rows and columns were clustered by the Euclidean distance. Statistical analysis was performed using t test error bars represent SEM and spearman correlation in heat map. *, $P < 0.05$; **, $P < 0.01$; ***, $P < 0.001$.

4. *Roseburia* spp. had different butyrate production rate and flagellin

Before investigating the effects of *Roseburia* on intestinal epithelial barrier function, *Roseburia* spp. were characterized to identify potential targets of the effects and possible strain-dependency. The genus *Roseburia* includes five species – *R. intestinalis, R. hominis, R. faecis, R. inulinivorans*, and *R. cecicola* [14]. Among them, three of *Roseburia* spp. were selected to subsequent experiments, based on closest phylogenetic distance (Fig. 4).

First of all, *Roseburia* is one of the butyrate-producing bacteria belong to Clostridium cluster XIVa. The growth curves and butyrate production rates of *Roseburia* spp. were compared (Fig. 5A-B). At 24h of culture, *R. faecis* generated the most amount of butyrate, followed by *R. hominis*, and *R. intestinalis* showed the lowest butyrate production. Second, *Roseburia*-derived flagellin had been recently studied that it acted as anti-inflammatory substance via regulating host HIF1α-AS gene in DSS-induced colitis mouse model [16]. By culturing in soft agar, motility was detected in all tested *Roseburia* spp. (Fig. 5C). And also, the presence of flagella was confirmed in transmission electron microscopy images (Fig. 5D). Then, flagellin extracts were isolated from cell pellet

of *Roseburia* spp. by centrifugation, and the size of flagellin fraction was compared on SDS-gel (Fig. 5E). *R. hominis* and *R. intestinalis*-derived flagellin proteins were comparable to each other in size, whereas that of *R. faecis* showed a distinct and larger size. Based on these comparisons among *Roseburia* spp., the supernatant in which butyrate is dissolved and flagellin extracts were further examined as the targets of interests.

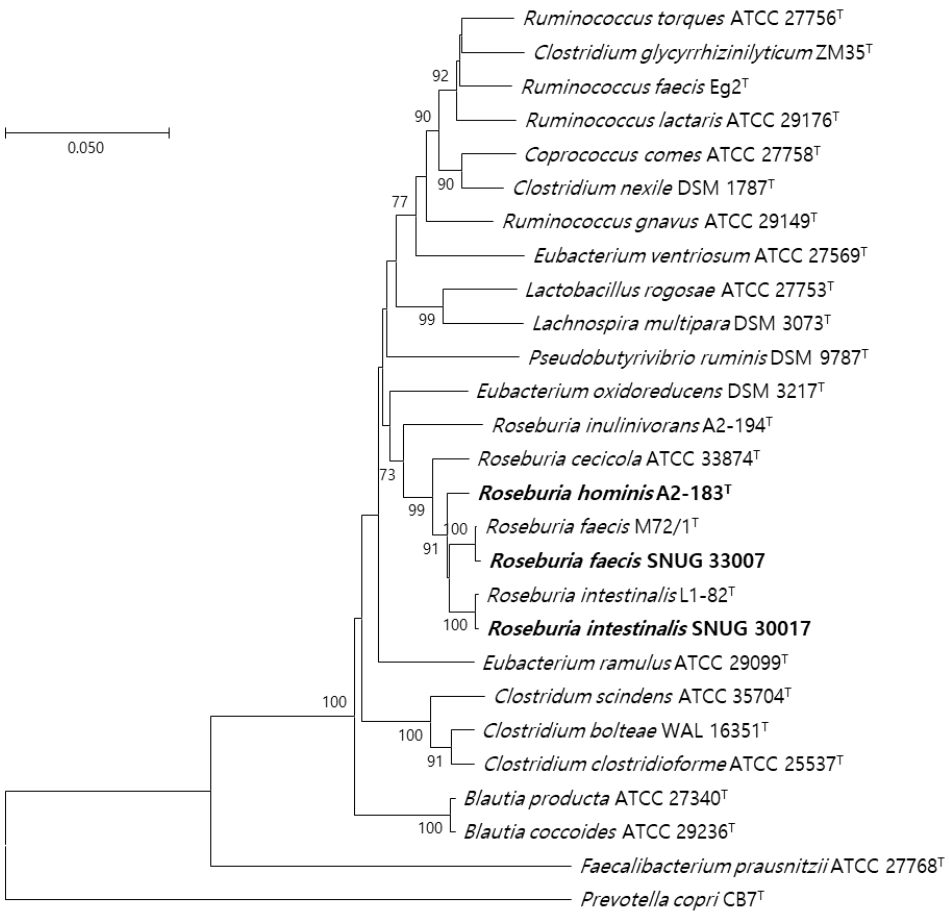
0.050
Ruminococcus torques ATCC 27756T
Clostridium glycyrrhizinilyticum ZM35T
Ruminococcus faecis Eg2T
Ruminococcus lactaris ATCC 29176T
Coprococcus comes ATCC 27758T
Clostridium nexile DSM 1787T
Ruminococcus gnavus ATCC 29149T
Eubacterium ventriosum ATCC 27569T
Lactobacillus rogosae ATCC 27753T
Lachnospira multipara DSM 3073T
Pseudobutyrivibrio ruminis DSM 9787T
Eubacterium oxidoreducens DSM 3217T
Roseburia inulinivorans A2-194T
Roseburia cecicola ATCC 33874T
Roseburia hominis A2-183T
Roseburia faecis M72/1T
Roseburia faecis SNUG 33007
Roseburia intestinalis L1-82T
Roseburia intestinalis SNUG 30017
Eubacterium ramulus ATCC 29099T
Clostridum scindens ATCC 35704T
Clostridium bolteae WAL 16351T
Clostridium clostridioforme ATCC 25537T
Blautia producta ATCC 27340T
Blautia coccoides ATCC 29236T
Faecalibacterium prausnitzii ATCC 27768T
Prevotella copri CB7T
92
90
90
77
99
73
99
100
91
100
100
100
91
100

Figure 4. Phylogenetic characterization of *Roseburia* spp. was shown and three of *Roseburia* spp. were chosen for subsequent experiments.

(A) Neighbour-joining tree based on 16S rRNA gene sequences of *Roseburia* spp. and related species. Numbers at branching points are percentages of bootstrap support (>70%) from 1,000 replications. Bar, 0.05 nt substitutions per position. Three of *Roseburia* spp. were highlighted in bold; two of them were not type species but the isolates.

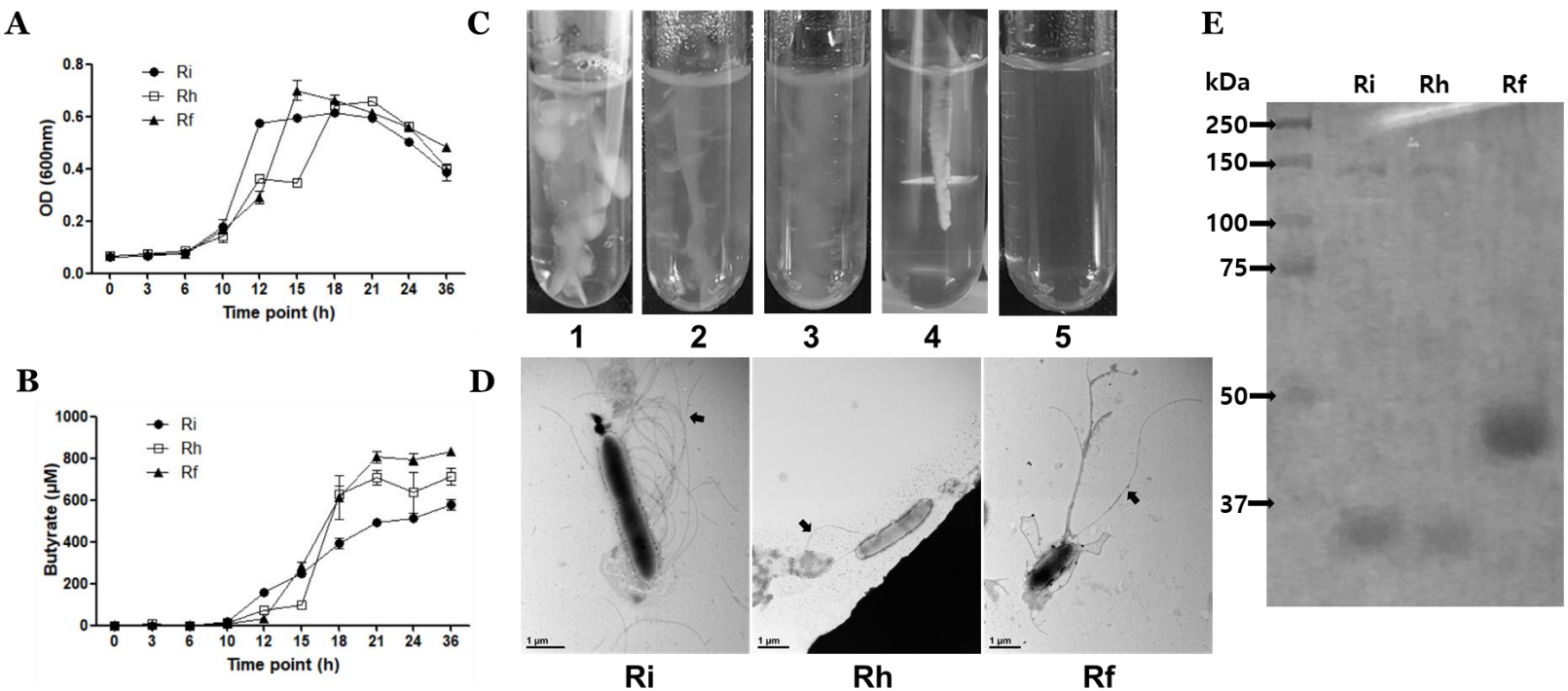
A
OD (600nm)
Time point (h)
Ri
Rh
Rf
B
Butyrate (μM)
Time point (h)
C
1
2
3
4
5
D
Ri
Rh
Rf
E
kDa
Ri
Rh
Rf
250
150
100
75
50
37

Figure 5. *Roseburia* spp. had different rate of butyrate production and size of flagellin proteins.

(A) Growth curves of *Roseburia* spp. were measured with 3h intervals. (B) Supernatants were collected at each time point and the rate of butyrate production was measured using GC-FID. (C) Motility was tested in YBHI soft agar medium (0.5% agar); 1, Ri, 2, Rh, 3, Rf, 4, *Lactobacillus ruminis* SNUG30021 (non-motile, control), 5, control medium. (D) Flagella (black arrow) were shown on TEM images; bar, 1μm (E) Flagellin protein was extracted and loaded on PAGE-GEL.

5. More than 3%(v/v) of ethanol concentration disrupted tight junction, but had no cell toxicity

To determine a suitable ethanol concentration to be used *in vitro* intestinal barrier disruption, different ethanol concentrations were tested on Caco-2 monolayer and tight junction-related protein levels and cell viability were measured by western blot and MTT assay, respectively (Fig. 6A-B). The protein levels of Occludin at different ethanol concentrations were decreased in dose-dependent manner, representing that more than 3% (v/v) of ethanol damaged tight junction. However, the concentration of ethanol did not affect Caco-2 cell viability, indicating the absence of cell toxicity. Therefore, it was selected as adequate ethanol concentration for further *in vitro* studies.

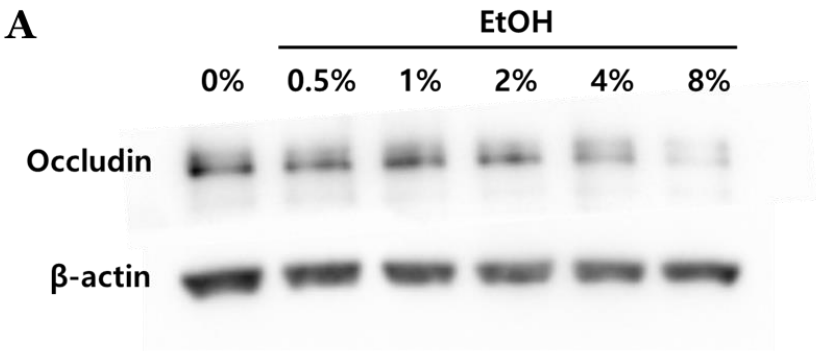
A
EtOH
0%
0.5%
1%
2%
4%
8%
Occludin
β-actin

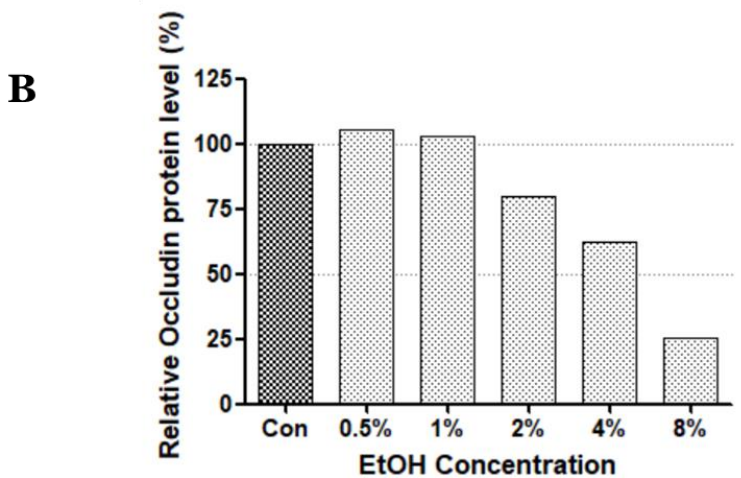
B
Relative Occludin protein level (%)
125
100
75
50
25
0
Con
0.5%
1%
2%
4%
8%
EtOH Concentration

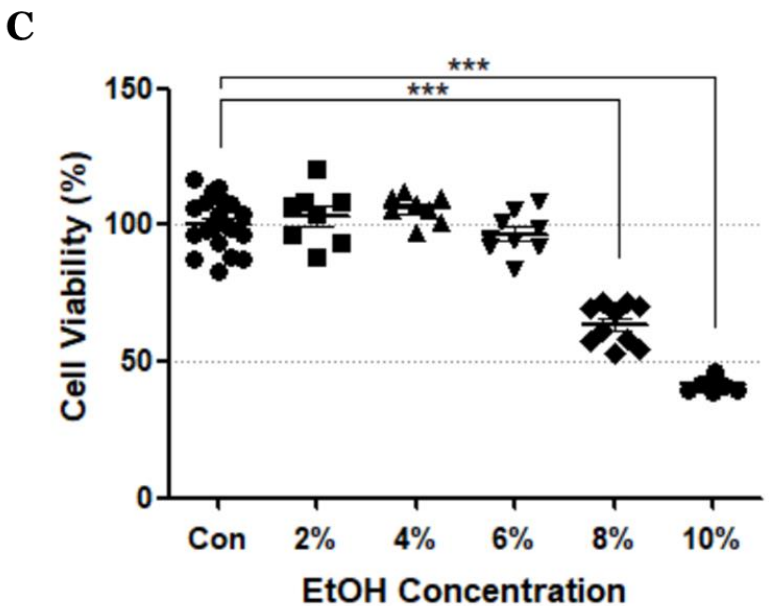
C
***
***
Cell Viability (%)
150
100
50
0
Con
2%
4%
6%
8%
10%
EtOH Concentration

Figure 6. More than 3% of ethanol concentration disrupted tight junction, but had no cell toxicity.

(A) Protein expression levels of Occludin was detected at different concentration of ethanol, and (B) quantified (Not performed statistics, n=1). (C) Cell viability of Caco-2 was measured with different concentrations of ethanol using MTT assay. Statistical analysis was performed using t test error bars represent SEM.

6. Live *Roseburia* bacteria treatment improve tight junction in ethanol-damaged Caco-2 monolayer

To analyze effect of live bacteria cell on intestinal epithelial tight junction, live *Roseburia* were treated to polarized Caco-2 monolayer on Transwell system. Live *Roseburia* improved relative TEER change after 24h (Fig. 7A). Subsequently, ethanol was challenged to examine the capability of live *Roseburia* to ameliorate tight junction disruption. Indeed, there was slightly enhancement of relative TEER change after ethanol exposure (Fig. 7B). Next, FITC-dextran was treated onto Caco-2 apical compartment to test permeability (Fig. 7C). Although relative TEER change minimally augmented after ethanol exposure, permeability was considerably normalized. This effect may result from enhancement of tight junction by live bacteria treatment for first 24h. Therefore, live *Roseburia* can enhance intestinal epithelial tight junction, although it could not protect directly ethanol-induced barrier dysfunction.

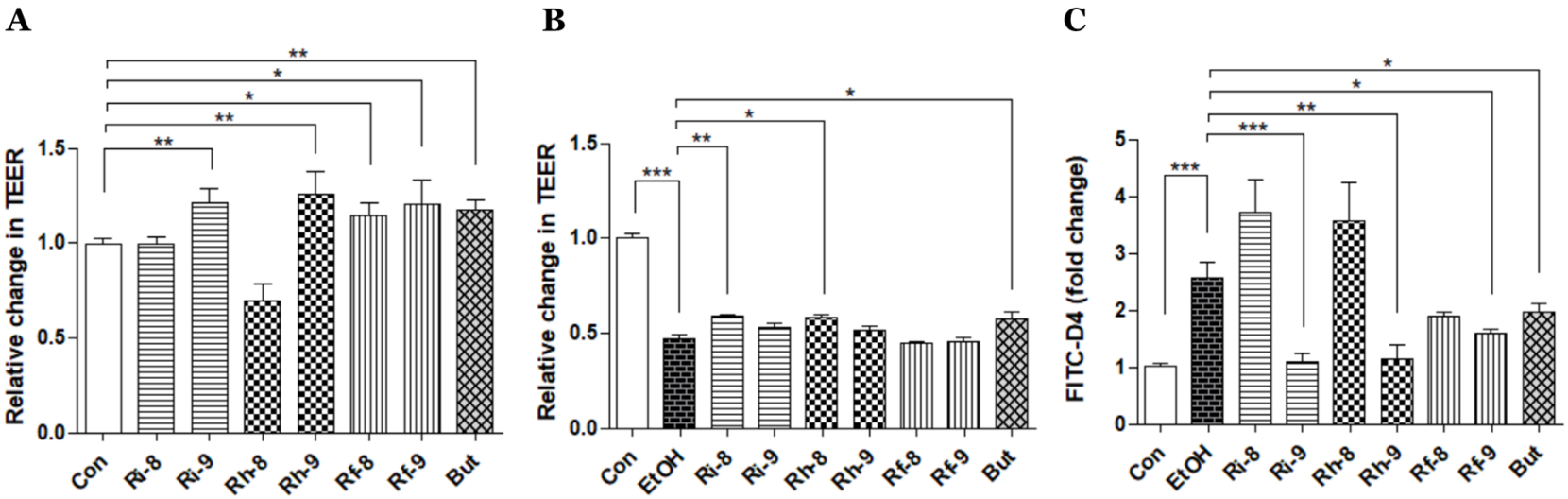
A
Relative change in TEER
1.5
1.0
0.5
0.0
**
**
*
*
**
Con
Ri-8
Ri-9
Rh-8
Rh-9
Rf-8
Rf-9
But
B
Relative change in TEER
1.5
1.0
0.5
0.0
***
**
*
*
Con
EtOH
Ri-8
Ri-9
Rh-8
Rh-9
Rf-8
Rf-9
But
C
FITC-D4 (fold change)
5
4
3
2
1
0
***
***
**
*
*
Con
EtOH
Ri-8
Ri-9
Rh-8
Rh-9
Rf-8
Rf-9
But

Figure 7. Live *Roseburia* spp. increased relative TEER change and mitigated permeability in ethanol-damaged Caco-2 monolayer.

In Caco-2 transwell system, (A) relative TEER change after live *Roseburia* spp. treatment at 10^8, 10^9 $cells/ml$ for 24h was measured. (B) 3% (v/v) of ethanol was challenged for 3h and relative TEER change was measured. (C) FITC-dextran was treated onto apical region at 1mg/ml for 1h and fluorescence was measured in basolateral region; measured the amount of FITC-dextran passed through the membrane. But, sodium butyrate (2mM, 1% v/v) as a positive control. Statistical analysis was performed using t test error bars represent SEM.

7. The supernatant from *Roseburia* spp. had no effects on strengthening tight junction in ethanol-damaged Caco-2 monolayer

As one of the possibility influencing intestinal epithelial barrier function, the supernatant, of which metabolites of *Roseburia* such as butyrate composed, was examined in this *in vitro* scheme. However, following administration of the supernatants for 24h, relative TEER change had not been enhanced, but even significantly reduced (Fig. 8A). TEER value was consistent or decreased after subsequent ethanol challenge (Fig. 8B). Finally, FITC-dextran permeability test clearly showed that the supernatant did not reinforce tight junction (Fig. 8C). Accordingly, it was evident that the supernatants had no effect on improving intestinal epithelial tight junction, although they contained butyrate.

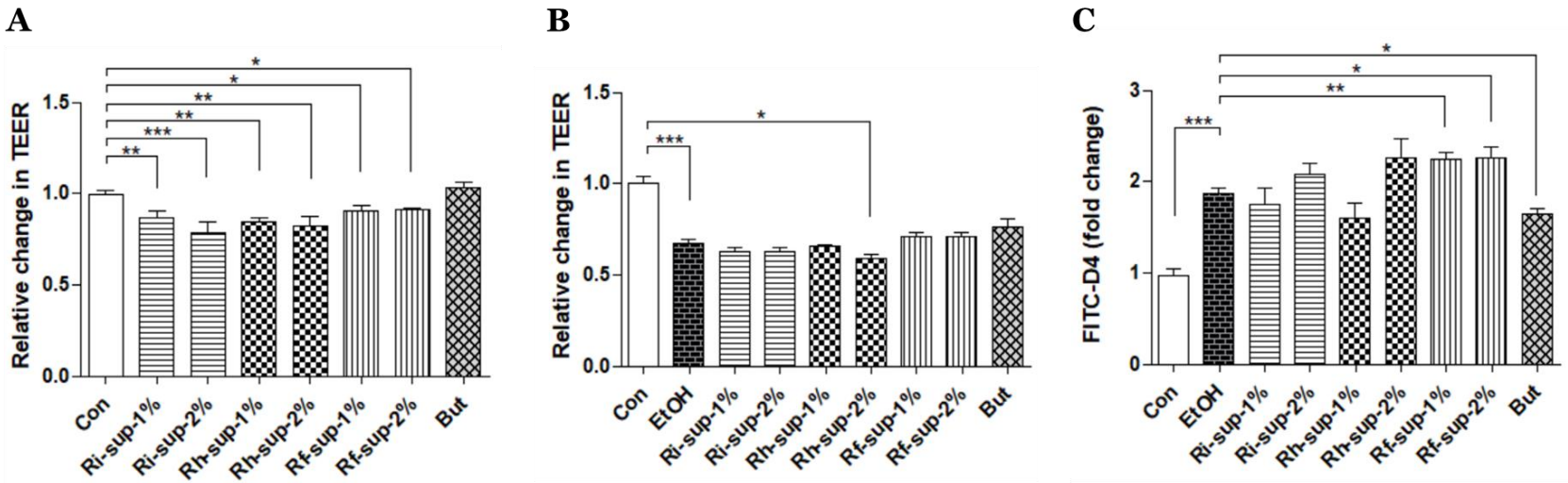
A
B
C
Relative change in TEER
FITC-D4 (fold change)
Con
EtOH
Ri-sup-1%
Ri-sup-2%
Rh-sup-1%
Rh-sup-2%
Rf-sup-1%
Rf-sup-2%
But

Figure 8. The supernatants from *Roseburia* spp. had no effects on strengthening tight junction in ethanol-damaged Caco-2 monolayer.

In Caco-2 transwell system, (A) relative TEER change after supernatant of *Roseburia* spp. treatment at 1, 2% (v/v) for 24h was measured. (B) Ethanol 3% (v/v) was challenged for 3h and relative TEER change was measured. (C) FITC-dextran was treated onto apical region at 1mg/ml for 1h and fluorescence was measured in basolateral region; measured the amount of FITC-dextran passed through the membrane. But, sodium butyrate (2mM, 1% v/v) as a positive control. Statistical analysis was performed using t test error bars represent SEM.

8. Flagellins derived from *Roseburia* spp. are differentially effective on tight junction in ethanol-damaged Caco-2 monolayer

The other possibility of beneficial effects of live *Roseburia* bacteria on enhancing Caco-2 tight junction was their flagellin. We examined *Roseburia*-derived flagellin extracts in this scheme. After flagellin extracts were treated for 24h, flagellin extracts from *R. intestinalis* and *R. hominis* (the former) significantly increased relative TEER change value, whereas that of *R. faecis* (the later) decreased the value (Fig. 9A). Moreover, the former reinforced tight junction following ethanol challenge, but the latter did not (Fig. 9B). Consistently, the former enhanced FITC-dextran permeability and the latter had no effects (Fig. 9C). Therefore, *Roseburia*-derived flagellin can enhance intestinal tight junction in ethanol-damaged Caco-2 monolayer in strain-dependent manner.

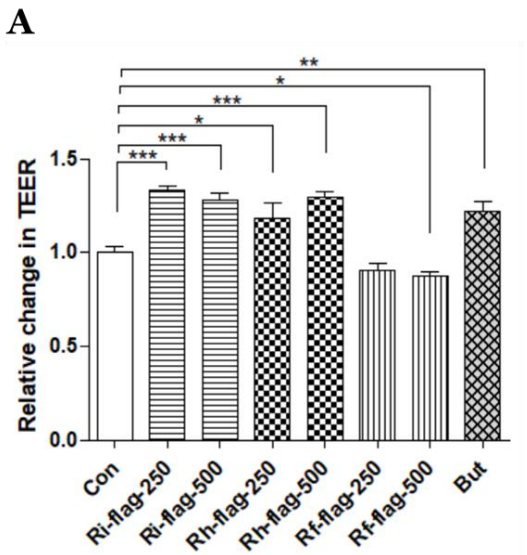
A
Relative change in TEER
1.5
1.0
0.5
0.0
***
***
*
***
*
**
Con
Ri-flag-250
Ri-flag-500
Rh-flag-250
Rh-flag-500
Rf-flag-250
Rf-flag-500
But

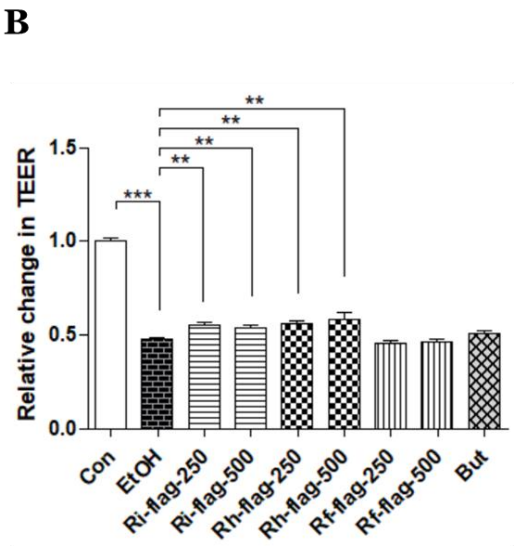
B
Relative change in TEER
1.5
1.0
0.5
0.0
***
**
**
**
**
Con
EtOH
Ri-flag-250
Ri-flag-500
Rh-flag-250
Rh-flag-500
Rf-flag-250
Rf-flag-500
But

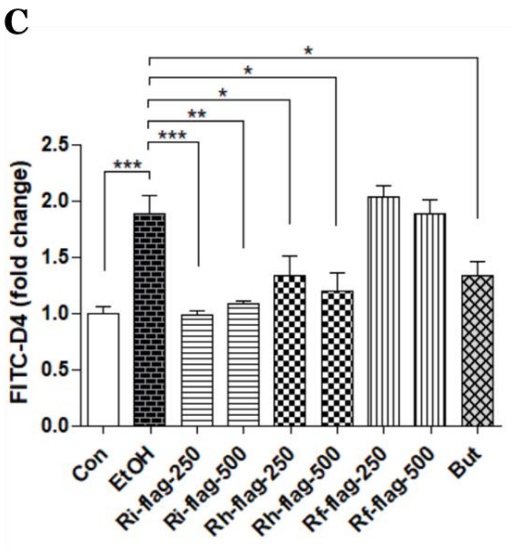
C
FITC-D4 (fold change)
2.5
2.0
1.5
1.0
0.5
0.0
***
**
*
*
*
Con
EtOH
Ri-flag-250
Ri-flag-500
Rh-flag-250
Rh-flag-500
Rf-flag-250
Rf-flag-500
But

Figure 9. Flagellin extracts derived from *R. intestinalis* and *R. hominis* increased relative TEER change and permeability in ethanol-damaged Caco-2 monolayer.

In transwell system, (A) relative TEER change after treatment of flagellin extracts derived from *Roseburia* spp. at 250, 500μg/ml for 24h was measured. (B) 3% of ethanol was challenged for 3h and relative TEER change was measured. (C) FITC-dextran was treated into apical region at 1mg/ml for an hour and fluorescence of FITC-dextran was measured in basolateral region; the amount of FITC-dextran transferred through membrane. But, sodium butyrate (2mM, 1% v/v) as a positive control. Statistical analysis was performed using t test error bars represent SEM.

IV. Discussion

In this study, we revealed three major findings. First, *Roseburia* was associated with expression levels of intestinal tight junction genes in ALD mice. Second, live *Roseburia* had a strengthening effects on ethanol-damaged Caco-2 monolayer. Third, protective effect of *Roseburia* on tight junctions in Caco-2 cell is partly derived from their flagellin with strain-specificity, rather than their metabolites. These findings suggested that *Roseburia* spp. were involved in regulation of ethanol-induced intestinal barrier dysfunction through their flagellin in strain-dependent manner.

ALD mouse model using Lieber-DeCarli diet clearly showed clinical ALD properties, such as elevated levels of serum ALT and AST, consistent with previous studies [7, 27]. Previous studies have been focused on gut barrier dysfunction in ALD [7, 28], since translocation of endotoxin has been proposed as one of the main causes. Likewise, we observed increased *in vivo* permeability and serum endotoxin levels in ethanol-fed group (Fig. 1F-G). Therefore, this ALD mouse model was well constructed to investigate association between gut microbiota and intestinal barrier function in ethanol-damaged condition.

It has been recently accepted that composition of gut microbiota is

altered in ALD [29]. For instance, the abundance of *Lactobacillus* was decreased in both ALD patients and mouse [30]. Also, administration of specific gut microbiota, such as *Lactobacillus* spp., enhanced gut barrier function [31], and subsequently alleviated ALD [7]. In this study, we focused on specific gut microbiota, *Roseburia*, of which abundance was significantly decreased in ALD mice (Fig. 3A). We investigated their protective effects on ethanol-damaged intestinal barrier, which is important in alleviation of ALD.

Gut microbiota analysis in ALD mice showed expansions of class *Gammaproteobacteria* and its family *Enterobacteriaceae*, which represent dysbiosis of gut microbiota not only in ALD but also in various pathological conditions [32-34]. This is because they are composed of Gram-negative bacteria such as *Salmonella*, *Shigella* and *Escherichia coli*, which all release endotoxins [35]. Consistently, we observed this altered gut microbial composition in the ethanol-fed group (Fig. 2C), and it may contribute to following endotoxemia (Fig. 1G). On the other hand, phylum *Bacteroidetes* and its genus *Bacteroides* were enriched in gut microbiota from pair-fed mice compared to ethanol-fed mice. It is well established that genus *Bacteroides* normally makes up great portion of mammalian intestinal microbiota and has beneficial effects in various diseases such as colon cancer [36, 37]. However, the family

Lachnospiraceae, which also observed as one of the significantly increased taxa in pair-fed mice (Fig. 2C), has been barely studied in ALD. In particular, genus *Roseburia*, which belongs to family *Lachnospiraceae*, has been also scarcely examined as target of probiotic effects in ALD. Therefore, we sought to figure out the effects of *Roseburia* on ALD and gut barrier function.

It has been demonstrated that alcohol consumption results in gut barrier dysfunction by disrupting tight junction [2]. Alcohol itself disrupts tight junction by not only generating reactive oxygen species (ROS), but also inhibiting the expression levels of tight junction-related genes such as Zo-1 and Occludin [1, 7]. In this study, the expression levels of Occludin were significantly decreased in ALD mice compared to pair-fed mice (Fig. 3B), and it was significantly correlated with the abundance of *Roseburia* (Fig. 3C), indicating the association with gut barrier function in ethanol-damaged condition. However, transcriptional expression levels were not sufficient to represent gut barrier function. Therefore, further evaluation of protein expression levels of tight junction is needed to confirm this *in vivo* finding. Nonetheless, it is undeniable that the evidence is worth to move on to Caco-2 *in vitro* experiments to figure out the effects of *Roseburia*.

Intestinal carcinoma Caco-2 monolayer has been adopted to examine

intestinal epithelial permeability using transwell system [11]. It simulates the structure of intestine effectively, as it structurally holds epithelial monolayer in between two compartments; upper one represents apical region and bottom represents basolateral region of intestine. Integrity of tight junction could be measured as TEER value between apical and basolateral region. Also paracellular permeability could be evaluated by passing fluorescence-labeled inulin or dextran through the Caco-2 monolayer [12]. Therefore, it is suitable *in vitro* system to analyze the effects of gut microbiota and their metabolites on epithelial barrier function. Furthermore, *Elhaseen E. Elamin et al.* modified the model to assess the intestinal epithelial permeability in ethanol-damaged condition, and demonstrated the protective effects of butyrate [13], which has been widely reported as beneficial metabolites in maintaining intestinal homeostasis [25]. We adopted this *in vitro* model to investigate effects of live *Roseburia* on ethanol-damaged gut barrier function (Fig. 7). Moreover, as well as live *Roseburia* cells, their metabolites and flagellin extracts were also evaluated to find the effector molecule in ALD (Fig. 8-9).

In this study, however, it is limited that relative change of TEER value was the only evidence for strengthened tight junction. Many studies demonstrated both TEER value and protein expression levels of tight

junction to substantiate the improving effects on gut barrier integrity [7, 10]. Thus, to clarify the effects of *Roseburia* on intestinal tight junction, more data should be supported, such as expression levels of tight junction-related mRNA genes or proteins in Caco-2 cells. Nonetheless, it is obvious that both TEER value and the subsequent permeability test are powerful evidence for evaluating gut barrier integrity.

As one of the butyrate-producing bacteria, *Roseburia* has been associated with various diseases, such as obesity, diabetes and colitis [14]. Recently, *Roseburia hominis* has been examined their anti-inflammatory effects on colitis mouse model [38], and so did *Roseburia intestinalis*-derived flagellin [16]. Therefore, strain-specific effects of *Roseburia* on health and disease should be understood. In this *in vitro* study, flagellin extracts from three *Roseburia* species improved ethanol-induced barrier dysfunction in strain-dependent manner (Fig. 9), whereas their metabolites did not show improving effects (Fig. 8). However, further study is needed to be performed to clarify the effect of flagellin, such as elucidating the mechanism of action in signaling pathways containing TLR5, which is known as a receptor for flagellin.

Flagellin is a globular protein forming the filament in a bacterial flagellum, rendering bacterial motility. It has been widely accepted as inflammatory molecules, like endotoxins. For instance, *Salmonella*-

derived flagellin clearly induces inflammation [39]. On the other hand, recently published study focused on immunomodulatory potency of flagellin derived from gut commensal [40]. In this context, we suggested *Roseburia*-derived flagellin plays a protective role in ethanol-induced Caco-2 barrier dysfunction. The conflicting potencies of flagellin may be derived from strain-dependent different structure of flagellin [41]. Indeed, size of flagellin fractions was different among *Roseburia* spp. and their strain-specific effects were observed. Thus, these findings could support understanding beneficial roles of flagellin in intestinal barrier function. However, it should be further evaluated whether these effects of *Roseburia*-derived flagellin are specific in ethanol-damaged condition or not. Since both *R. hominis* and *R. intestinalis* were shown to alleviate colitis, which are representative to gut barrier dysfunction [16, 38], it may possible that both effects were partly derived from their flagellin.

In conclusion, this study showed novel association between particular gut microbiota, *Roseburia*, and gut barrier dysfunction in ALD mice. Moreover, protective effects of *Roseburia* on ethanol-damaged Caco-2 monolayer were investigated, and the effector molecule of *Roseburia* was suggested as their flagellin with strain-specificity. In order to substantiate the causal effects of *Roseburia*, *Roseburia*-fed ALD mouse

model should be constructed in the future study. Consequently, *Roseburia* and their flagellin could be novel therapeutic targets of ALD.

V. References

1. Louvet A, Mathurin P. Alcoholic liver disease: mechanisms of injury and targeted treatment. Nat Rev Gastroenterol Hepatol. 2015;12(4):231-42. doi: 10.1038/nrgastro.2015.35. PubMed PMID: 25782093.
2. Szabo G. Gut-liver axis in alcoholic liver disease. Gastroenterology. 2015;148(1):30-6. doi: 10.1053/j.gastro.2014.10.042. PubMed PMID: 25447847; PubMed Central PMCID: PMCPMC4274189.
3. Roh YS, Seki E. Toll-like receptors in alcoholic liver disease, non-alcoholic steatohepatitis and carcinogenesis. J Gastroenterol Hepatol. 2013;28 Suppl 1:38-42. doi: 10.1111/jgh.12019. PubMed PMID: 23855294; PubMed Central PMCID: PMCPMC3721430.
4. Wang B, Yao M, Lv L, Ling Z, Li L. The Human Microbiota in Health and Disease. Engineering. 2017;3(1):71-82. doi: 10.1016/j.eng.2017.01.008.
5. Goel A, Gupta M, Aggarwal R. Gut microbiota and liver disease. Journal of Gastroenterology and Hepatology. 2014;29(6):1139-48. doi: 10.1111/jgh.12556. PubMed PMID: WOS:000335973300007.
6. Mutlu EA, Gillevet PM, Rangwala H, Sikaroodi M, Naqvi A, Engen PA, et al. Colonic microbiome is altered in alcoholism. Am J Physiol Gastrointest Liver Physiol. 2012;302(9):G966-78. doi: 10.1152/ajpgi.00380.2011. PubMed PMID: 22241860; PubMed Central PMCID: PMCPMC3362077.
7. Wang Y, Kirpich I, Liu Y, Ma Z, Barve S, McClain CJ, et al. *Lactobacillus rhamnosus* GG treatment potentiates intestinal hypoxia-inducible factor, promotes intestinal integrity and ameliorates alcohol-induced liver injury. Am J Pathol. 2011;179(6):2866-75. doi: 10.1016/j.ajpath.2011.08.039. PubMed PMID: 22093263; PubMed Central PMCID: PMCPMC3260853.
8. Tian F, Chi F, Wang G, Liu X, Zhang Q, Chen Y, et al. *Lactobacillus rhamnosus* CCFM1107 treatment ameliorates alcohol-induced liver injury in a mouse model of chronic alcohol feeding. J Microbiol. 2015;53(12):856-63. doi: 10.1007/s12275-015-5239-5. PubMed PMID: 26626356.
9. Gonzalez-Mariscal L, Tapia R, Chamorro D. Crosstalk of tight junction components with signaling pathways. Biochim Biophys Acta. 2008;1778(3):729-56. doi: 10.1016/j.bbamem.2007.08.018. PubMed PMID: 17950242.
10. Wang Y, Tong J, Chang B, Wang B, Zhang D, Wang B. Effects of alcohol on intestinal epithelial barrier permeability and expression of tight junction-associated proteins. Mol Med Rep. 2014;9(6):2352-6. doi: 10.3892/mmr.2014.2126. PubMed PMID: 24718485.
11. Hidalgo IJ, Raub TJ, Borchardt RT. Characterization of the Human Colon Carcinoma Cell Line (Caco-2) as a Model System for Intestinal Epithelial Permeability. Gastroenterology. 1989;96(2):736-49. doi: 10.1016/s0016-5085(89)80072-1.
12. Srinivasan B, Kolli AR, Esch MB, Abaci HE, Shuler ML, Hickman JJ. TEER measurement techniques for in vitro barrier model systems. J Lab Autom. 2015;20(2):107-26. doi: 10.1177/2211068214561025. PubMed PMID: 25586998; PubMed Central PMCID: PMCPMC4652793.
13. Elamin EE, Masclee AA, Dekker J, Pieters HJ, Jonkers DM. Short-chain fatty acids activate AMP-activated protein kinase and ameliorate ethanol-induced intestinal barrier dysfunction in Caco-2 cell monolayers. J Nutr. 2013;143(12):1872-81. doi: 10.3945/jn.113.179549. PubMed PMID: 24132573.
14. Tamanai-Shacoori Z, Smida I, Bousarghin L, Loreal O, Meuric V, Fong SB,

et al. *Roseburia* spp.: a marker of health? Future microbiology. 2017;12:157-70. Epub 2017/02/01. doi: 10.2217/fmb-2016-0130. PubMed PMID: 28139139.
15. Hamer HM, Jonkers D, Venema K, Vanhoutvin S, Troost FJ, Brummer RJ. Review article: the role of butyrate on colonic function. Aliment Pharmacol Ther. 2008;27(2):104-19. doi: 10.1111/j.1365-2036.2007.03562.x. PubMed PMID: 17973645.
16. Quan Y, Song K, Zhang Y, Zhu C, Shen Z, Wu S, et al. *Roseburia intestinalis*-derived flagellin is a negative regulator of intestinal inflammation. Biochem Biophys Res Commun. 2018;501(3):791-9. doi: 10.1016/j.bbrc.2018.05.075. PubMed PMID: 29772233.
17. Ferrere G, Wrzosek L, Cailleux F, Turpin W, Puchois V, Spatz M, et al. Fecal microbiota manipulation prevents dysbiosis and alcohol-induced liver injury in mice. J Hepatol. 2017;66(4):806-15. doi: 10.1016/j.jhep.2016.11.008. PubMed PMID: 27890791.
18. Bertola A, Mathews S, Ki SH, Wang H, Gao B. Mouse model of chronic and binge ethanol feeding (the NIAAA model). Nat Protoc. 2013;8(3):627-37. doi: 10.1038/nprot.2013.032. PubMed PMID: 23449255; PubMed Central PMCID: PMCPMC3788579.
19. Folch J, Lees M, Sloane Stanley GH. A simple method for the isolation and purification of total lipides from animal tissues. The Journal of biological chemistry. 1957;226(1):497-509. Epub 1957/05/01. PubMed PMID: 13428781.
20. Ramirez-Farias C, Slezak K, Fuller Z, Duncan A, Holtrop G, Louis P. Effect of inulin on the human gut microbiota: stimulation of *Bifidobacterium adolescentis* and *Faecalibacterium prausnitzii*. Br J Nutr. 2009;101(4):541-50. doi: 10.1017/S0007114508019880. PubMed PMID: 18590586.
21. Bae MJ, Shin HS, See HJ, Jung SY, Kwon DA, Shon DH. Baicalein induces CD4(+)Foxp3(+) T cells and enhances intestinal barrier function in a mouse model of food allergy. Sci Rep. 2016;6:32225. doi: 10.1038/srep32225. PubMed PMID: 27561877; PubMed Central PMCID: PMCPMC4999817.
22. Tsai PY, Zhang B, He WQ, Zha JM, Odenwald MA, Singh G, et al. IL-22 Upregulates Epithelial Claudin-2 to Drive Diarrhea and Enteric Pathogen Clearance. Cell Host Microbe. 2017;21(6):671-81 e4. doi: 10.1016/j.chom.2017.05.009. PubMed PMID: 28618266; PubMed Central PMCID: PMCPMC5541253.
23. Seo B, Yoo JE, Lee YM, Ko G. *Merdimonas faecis* gen. nov., sp. nov., isolated from human faeces. Int J Syst Evol Microbiol. 2017;67(7):2430-5. doi: 10.1099/ijsem.0.001977. PubMed PMID: 28741995.
24. David LA, Maurice CF, Carmody RN, Gootenberg DB, Button JE, Wolfe BE, et al. Diet rapidly and reproducibly alters the human gut microbiome. Nature. 2014;505(7484):559-63. doi: 10.1038/nature12820. PubMed PMID: 24336217; PubMed Central PMCID: PMCPMC3957428.
25. Peng L, Li ZR, Green RS, Holzman IR, Lin J. Butyrate enhances the intestinal barrier by facilitating tight junction assembly via activation of AMP-activated protein kinase in Caco-2 cell monolayers. J Nutr. 2009;139(9):1619-25. doi: 10.3945/jn.109.104638. PubMed PMID: 19625695; PubMed Central PMCID: PMCPMC2728689.
26. Million M, Tomas J, Wagner C, Lelouard H, Raoult D, Gorvel J-P. New insights in gut microbiota and mucosal immunity of the small intestine. Human Microbiome Journal. 2018;7-8:23-32. doi: https://doi.org/10.1016/j.humic.2018.01.004.
27. Xu MJ, Cai Y, Wang H, Altamirano J, Chang B, Bertola A, et al. Fat-Specific

Protein 27/CIDEC Promotes Development of Alcoholic Steatohepatitis in Mice and Humans. Gastroenterology. 2015;149(4):1030-41 e6. doi: 10.1053/j.gastro.2015.06.009. PubMed PMID: 26099526; PubMed Central PMCID: PMCPMC4584194.
28. Rao R. Endotoxemia and gut barrier dysfunction in alcoholic liver disease. Hepatology. 2009;50(2):638-44. doi: 10.1002/hep.23009. PubMed PMID: 19575462; PubMed Central PMCID: PMCPMC6209509.
29. Hartmann P, Seebauer CT, Schnabl B. Alcoholic liver disease: the gut microbiome and liver cross talk. Alcohol Clin Exp Res. 2015;39(5):763-75. doi: 10.1111/acer.12704. PubMed PMID: 25872593; PubMed Central PMCID: PMCPMC4402724.
30. Scarpellini E, Forlino M, Lupo M, Rasetti C, Fava G, Abenavoli L, et al. Gut Microbiota and Alcoholic Liver Disease. Reviews on recent clinical trials. 2016;11(3):213-9. Epub 2016/08/16. PubMed PMID: 27515958.
31. Anderson RC, Cookson AL, McNabb WC, Park Z, McCann MJ, Kelly WJ, et al. *Lactobacillus plantarum* MB452 enhances the function of the intestinal barrier by increasing the expression levels of genes involved in tight junction formation. BMC microbiology. 2010;10:316. Epub 2010/12/15. doi: 10.1186/1471-2180-10-316. PubMed PMID: 21143932; PubMed Central PMCID: PMCPMC3004893.
32. Xu MJ, Zhou Z, Parker R, Gao B. Targeting inflammation for the treatment of alcoholic liver disease. Pharmacol Ther. 2017. doi: 10.1016/j.pharmthera.2017.06.007. PubMed PMID: 28642119.
33. Marlene R. Abundance and Diversity of Microbiota in Type 2 Diabetes and Obesity. Journal of Diabetes & Metabolism. 2013;04(03). doi: 10.4172/2155-6156.1000253.
34. Cassard AM, Ciocan D. Microbiota, a key player in alcoholic liver disease. Clin Mol Hepatol. 2018;24(2):100-7. doi: 10.3350/cmh.2017.0067. PubMed PMID: 29268595; PubMed Central PMCID: PMCPMC6038939.
35. Octavia S, Lan R. The Family *Enterobacteriaceae*. In: Rosenberg E, DeLong EF, Lory S, Stackebrandt E, Thompson F, editors. The Prokaryotes: Gammaproteobacteria. Berlin, Heidelberg: Springer Berlin Heidelberg; 2014. p. 225-86.
36. Wexler AG, Goodman AL. An insider's perspective: *Bacteroides* as a window into the microbiome. Nat Microbiol. 2017;2:17026. doi: 10.1038/nmicrobiol.2017.26. PubMed PMID: 28440278; PubMed Central PMCID: PMCPMC5679392.
37. Tsuruya A, Kuwahara A, Saito Y, Yamaguchi H, Tsubo T, Suga S, et al. Ecophysiological consequences of alcoholism on human gut microbiota: implications for ethanol-related pathogenesis of colon cancer. Sci Rep. 2016;6:27923. doi: 10.1038/srep27923. PubMed PMID: 27295340; PubMed Central PMCID: PMCPMC4904738.
38. Patterson AM, Mulder IE, Travis AJ, Lan A, Cerf-Bensussan N, Gaboriau-Routhiau V, et al. Human Gut Symbiont *Roseburia hominis* Promotes and Regulates Innate Immunity. Front Immunol. 2017;8:1166. doi: 10.3389/fimmu.2017.01166. PubMed PMID: 29018440; PubMed Central PMCID: PMCPMC5622956.
39. Hayashi F, Smith KD, Ozinsky A, Hawn TR, Yi EC, Goodlett DR, et al. The innate immune response to bacterial flagellin is mediated by Toll-like receptor 5. Nature. 2001;410(6832):1099-103. Epub 2001/04/27. doi: 10.1038/35074106. PubMed PMID: 11323673.
40. Hajam IA, Dar PA, Shahnawaz I, Jaume JC, Lee JH. Bacterial flagellin-a potent immunomodulatory agent. Exp Mol Med. 2017;49(9):e373. doi:

10.1038/emm.2017.172. PubMed PMID: 28860663; PubMed Central PMCID: PMCPMC5628280.
41. Lawn AM. Comparison of the flagellins from different flagellar morphotypes of *Escherichia coli*. Journal of general microbiology. 1977;101(1):112-30. Epub 1977/07/01. doi: 10.1099/00221287-101-1-121. PubMed PMID: 330818.

국문초록

로제부리아 균주의 알코올성 간질환과 장내 방벽에 대한 효과

서울대학교 보건대학원
환경보건학과 환경보건학 전공
전경찬

지도교수 고 광 표

알코올성 간질환은 알코올 섭취에 의해 무너진 장벽을 통해 장내의 내독소가 간으로 이동하여 염증을 일으킴으로써 발생할 수 있는데, 이러한 통로와 기작을 장-간 축이라 한다. 장내 미생물은 여러 질환에서 무너진 장벽을 강화시킬 수 있다고 보고 되어 있다. 하지만 알코올성 간질환에서 특정 장내 미생물의 장벽 기능과 질환 개선에 대하여는 연구가 미비한 실정이다. 본 연구에서는 먼저 알코올성 간질환 마우스 모델에서 장내 로제부리아의 수가 줄어들고, 이 수가 장내 밀착연접 단백질의 유전자 발현량과 상관 관계가 있음을 확인하였다. 따라서, 장내 로제부리아가 알코올에 의해 파괴된 장내 밀착 연접을 조절하는 데 잠재적인 역할을 할 것이라고 가정하였다. 로제부리아의 장내 밀착 연접에 대한 효과를 확인하기 위하여 *in vitro* 실험을 진행하였다. 로제부리아 생균의 처리가 Caco-2 인체 장벽 세포에서 밀착 연접을 강화시키고, 이후의 알코올 처리에 의해 증가된 장벽 투과성을 완화시킨다는 것을 확인하였다. 더 나아가, 로제부리아 속에 속하는 세 가지 종을 선택하여 그 특성을 분석한 결과, 부티르산 생산성 및 편모 단백질의 크기에 있어서 종 간 특이성이 있음을 확인하였다. 그리고 흥미롭게도, 편모 추출물은 Caco-2세

포에서 종 간 차이를 보이며 밀착 연접 강화 및 투과성 완화 효과를 보였다. 반면 부티르산이 대사체로서 들어 있는 로제부리아의 배양액은 밀착 연접 강화 및 투과성 완화에 대한 효과가 없는 것을 확인하였다. 따라서 로제부리아는 알코올에 의해 파괴된 장벽의 기능을 보호하는 효과를 보이고, 편모가 그 영향에 있어서 종 간의 차이를 보이며 관여할 수 있음을 밝혀내었다. 이러한 발견은 장내 미생물 로제부리아가 알코올성 간질환에 대한 새로운 프로바이오틱스 후보 균주가 될 수 있음을 시사한다.

주요 단어:, 로제부리아, 알코올성 간질환, 편모, 뷰티르산, Caco-2, 인체 장벽 세포, 알코올, 밀착 연접, 장내 미생물

학번: 2017-29583